

**Thirteenth Quarterly Progress Report**

August 1, 2009 to October 31, 2009

Contract No. HHS-N-260-2006-00005-C

***Neurophysiological Studies of Electrical Stimulation for the Vestibular Nerve***

Submitted by:

James O. Phillips, Ph.D.<sup>1,3,4</sup>

Steven Bierer, Ph.D.<sup>1,3,4</sup>

Albert F. Fuchs, Ph.D.<sup>2,3,4</sup>

Chris R.S. Kaneko, Ph.D.<sup>2,3</sup>

Leo Ling, Ph.D.<sup>2,3</sup>

Shawn Newlands, M.D., Ph.D.<sup>5</sup>

Kaibao Nie, Ph.D.<sup>1,4</sup>

Jay T. Rubinstein, M.D., Ph.D.<sup>1,4,6</sup>

<sup>1</sup> Department of Otolaryngology-HNS, University of Washington, Seattle, Washington

<sup>2</sup> Department of Physiology and Biophysics, University of Washington, Seattle, Washington

<sup>3</sup> Washington National Primate Research Center, University of Washington, Seattle, Washington

<sup>4</sup> Virginia Merrill Bloedel Hearing Research Center, University of Washington, Seattle, Washington

<sup>5</sup> Department of Otolaryngology, University of Rochester, Rochester, New York

<sup>6</sup> Department of Bioengineering, University of Washington, Seattle, Washington

---

Reporting Period: August 1, 2009 to October 31, 2009

***Challenges:***

**1. We ended our experiments with multiple single unit axial recording electrodes from NeuroNexus – FHC.** No further electrodes have been forthcoming from NeuroNexus FHC and the two oversize electrodes that were provided did not produce good recordings. We tried plating the recording sites with iron in an attempt to improve the signal to noise ratio of the recordings, but this was not successful. In addition, the axial array proved very brittle, and both broke and delaminated from the tungsten electrode core after only a few tracks. Finally, the electrodes were large and had a broad flattened surface. These electrodes produced nystagmus when they were advanced into the brainstem, indicating that they cause significant damage to brainstem circuits as they are advanced (see below).

In response to these observations, we have abandoned the Neuronexus-FHC electrodes in favor of a new Thomas Recording tetrode design, with a non-pulled tip. These electrodes have given us a measure of success in recent brainstem recording despite the rather close spacing of the recording sites. Also, we have begun working with Dr. Satinderpall Singh Pannu of Lawrence Livermore National Laboratory on a new multiple single unit deep brain recording electrode design through a new initiative at NIDCD. Dr. Pannu is working on an electrode of his design, with specifications provided by our group. The new electrode will have four electrode recording sites in addition to the tip of the electrode, 25  $\mu\text{m}$  in diameter, separated by 250  $\mu\text{m}$ , along the axial length of a tungsten wire. This device should provide the size advantage of tetrodes, with the site spacing of the axial arrays.

**2. We are still mapping chambers and training monkeys.** Our new three-year protocol requires us to fully map the chambers prior to implantation of the stimulation device. We are performing our experiments in three steps. We are implanting eye coil and stabilization lugs. We are then training the monkeys to perform both head unrestrained and head restrained tracking behavior with and without background optokinetic visual motion and/or chair rotation. We then implant the recording chambers, and fully map the chambers with single unit recording techniques. Finally, we implant the prosthesis, perform canal plugging or gentamicin injection, and conduct stimulation studies. In the short term, this has altered the sequence of our recording and stimulation experiments. It also means that three new animals will likely come on line for stimulation and recording experiments at the same time, which is a logistical challenge.

To address this challenge we are pushing to complete as many experiments with our currently implanted animals as we can while we wait for our next implantations. Some of our current animals will be sacrificed when the new animals come on line in Quarter 14, and we hope to have approval for a series of histology experiments in collaboration with a group from the University of Melbourne at the same time.

***Current Successes:***

**1. In Quarter 13 we received the FDA response to our pre-IDE submission for a clinical trial of the vestibular prosthesis developed under this contract.** The review was very thorough but positive overall. We believe that we have successfully addressed the issues raised in the written FDA response in preparation for the submission of a full IDE application.

**2. We submitted abstracts for presentation of our results at several meetings.**

*Suppression of nystagmus with an implanted vestibular neurostimulator.* Jay Rubinstein, James Phillips, Leo Ling, Kaibao Nie. 7th Asia Pacific Symposium on Cochlear Implants and Related Sciences, Singapore, 2009

*Characterization of the Electrically-Evoked Compound Action Potential of the Vestibular Nerve.* Kaibao Nie, Steven Bierer, Leo Ling, Trey Oxford, James Phillips, Jay Rubinstein. American Otological Society, 2010, Las Vegas, NV. *This paper was selected as the first scientific presentation of the meeting.*

*Evaluation of a chronically implanted prosthesis to parametrically control nystagmic eye movements.* James Phillips, Leo Ling, Albert Fuchs, Chris Kaneko, Steven Bierer, Kaibao Nie, Trey Oxford, Shawn Newlands, Jay Rubinstein. Association for Research in Vision and Ophthalmology, 2010. Ft. Lauderdale, FL

*Recording of secondary vestibular neurons during electrical stimulation with a vestibular implant for the treatment of Meniere's disease.* Phillips, J.O., Ling, L., Fuchs, A.F., Oxford, T., Bierer, S.M., Nie, K., Kaneko, C, Newlands, S., Rubinstein, J.T. Sixth International Symposium on Meniere's Disease and Inner Ear Disorders. 2010, Kyoto, Japan.

**3. We presented our work at the society for Neuroscience Annual Meeting in Chicago, IL**

**4. We continued our rotational and electrical stimulation interaction studies.** We first created a vestibular stimulus that could produce a constant slow phase velocity vestibular nystagmus. This stimulus consisted of a rapid acceleration followed by a slow acceleration, which then reversed (sinusoidal ramp, 5 s half cycle, to 40 deg/s, then accelerate at 5 deg/s/s for 8 s). This was presented to the animals repeatedly, with and without electrical stimulation. This stimulus and the resulting eye movements are shown in Figure 1. During the combined stimulation studies, we monitored the slow phase eye velocity produced by the rotational stimulation in Figure 1, and applied electrical stimulation with a current and frequency that we predicted would match the observed velocity of the slow phases (300 pps, 150  $\mu$ A, 100 $\mu$ s pulse width, 8  $\mu$ s gap, E6 vs. ECEM1 & 2, lateral canal). We based our calculation on the original frequency and amplitude vs velocity curves for the implanted canal generated in a previous recording session.

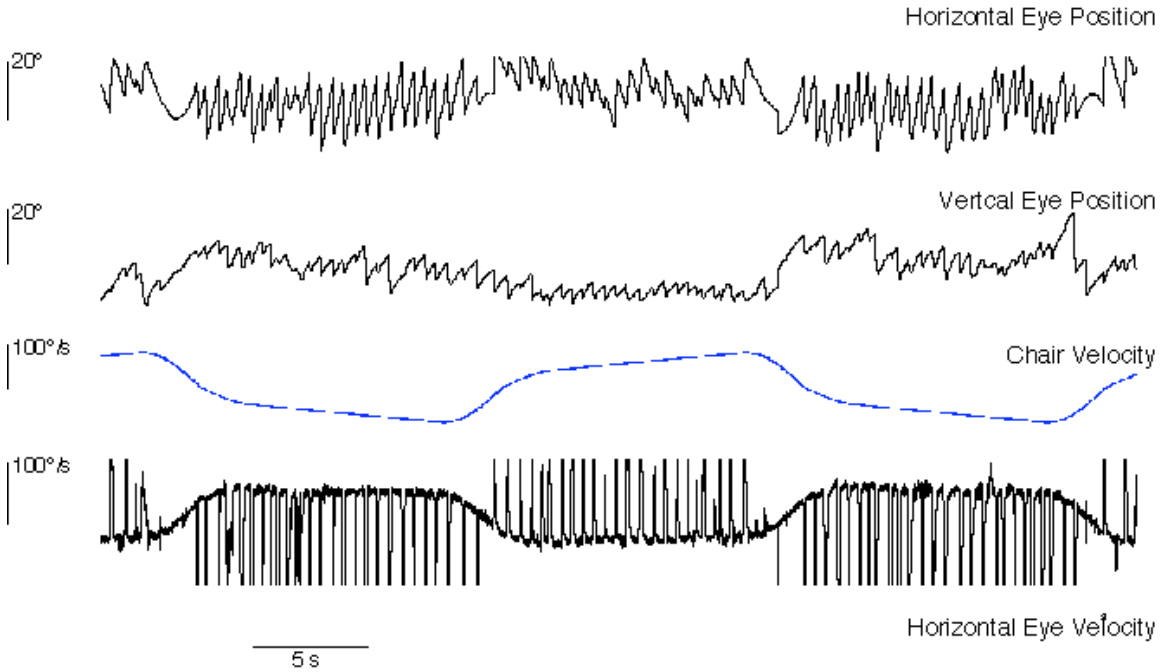


Figure 1. Vestibular stimulus that creates consistent slow phase velocity eye movements.

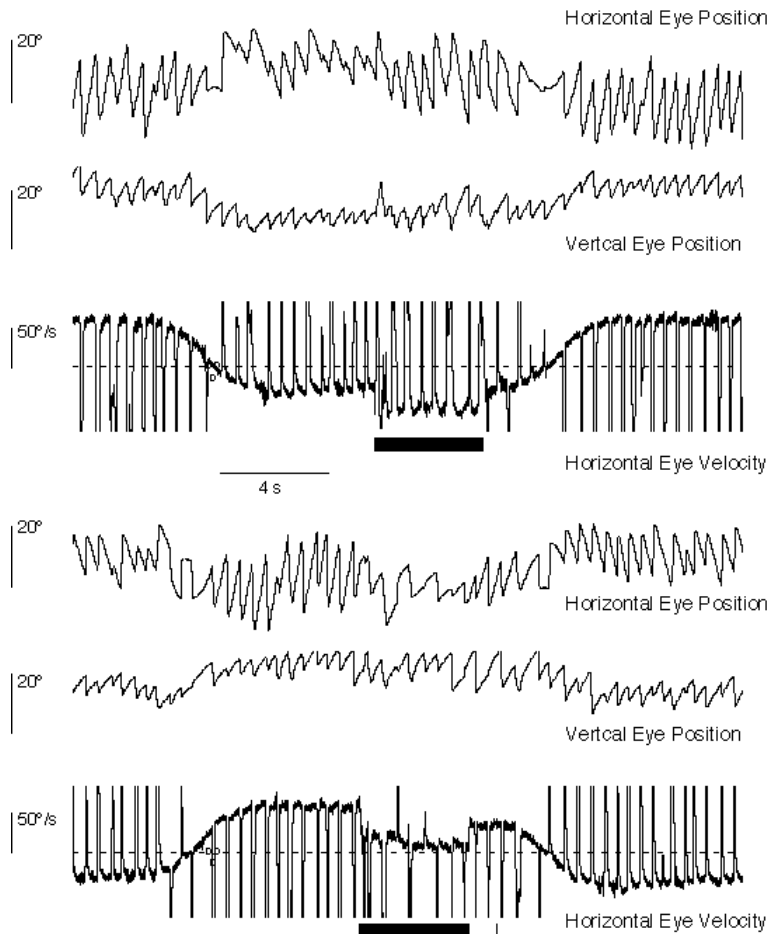


Figure 2: Doubling and nulling of vestibular nystagmus with electrical stimulation.

The result, illustrated in Figure 2, is a reduction in slow phase velocity toward the implanted canal, and an increase in slow phase velocity away from the implanted canal. Indeed, the velocity was nearly 0 deg/s in the direction of the implanted canal, and roughly twice the rotationally elicited velocity away from the implanted canal.

This result suggested that we should be able to use modulated real time stimulation to change the gain of the VOR. Since the frequency/current vs slow phase velocity curves estimated the velocity of VOR that we could cancel with electrical stimulation, we predicted that we could use modulation of one parameter to compensate for a constantly changing vestibular velocity signal. In Figure 3, we demonstrated that we can use real time modulated input from the clinical processor to null the vestibular nystagmus resulting from en-block sinusoidal rotation. In these experiments, we differentiated a real time head position signal and used that velocity signal to modulate the amplitude of a 1 KHz carrier that was sent to the direct audio input of a clinical processor. The processor then generated a 250 Hz stimulus train with an amplitude that was modulated by the amplitude of the input signal. We showed that increasing the gain of the modulated input signal decreased the gain of the VOR, when the signal was derived from head velocity in the plane of the stimulated canal and away from the implanted ear.

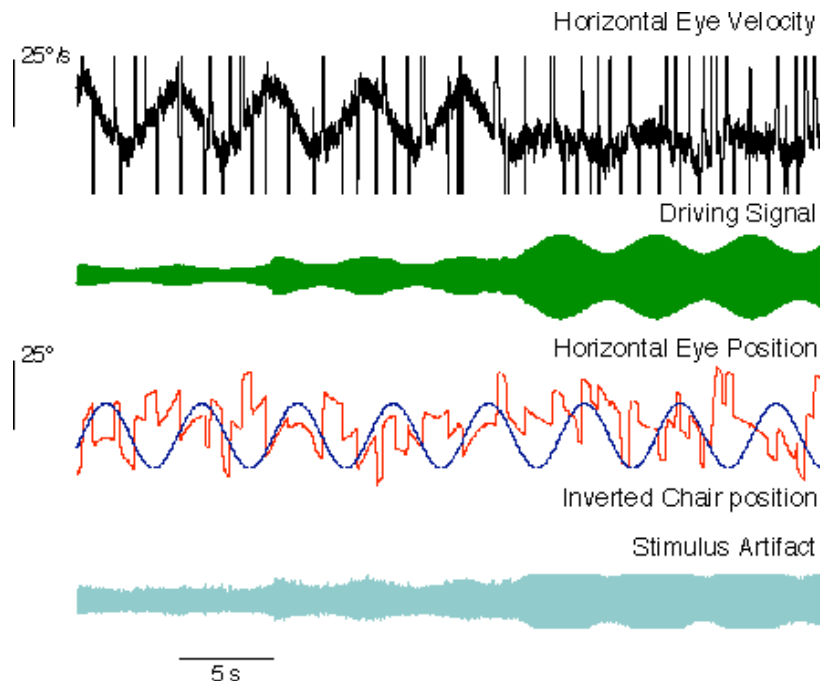


Figure 3: Modulation of vestibulo-ocular reflex with real time amplitude modulated electrical stimulation.

**5. We studied the interaction between rotational stimuli and volitional task performance with and without electrical stimulation.** In our experiments, we required the animal to pursue a sinusoidally moving point target ( $0.22 \text{ Hz} \pm 10 \text{ deg}$ ) while being subjected to en-bloc rotation in the dark. The rotational stimulus was the same as that in

Figure 1. The resulting eye movements showed a robust nystagmus superimposed on the smooth pursuit eye movements. When electrical stimulation was applied to the lateral canal, the nystagmus was decreased and the pursuit eye movements became more accurate, as can be seen in Figure 4. The timing of this response differed from the timing of the response to electrical stimulation in the dark, shown in Figure 2. The optimal pursuit performance followed the onset of stimulation in all trials. This suggests that the perceptual experience of the electrical stimulation, and the resulting restoration of volitional pursuit behavior, may lag the reflex response to the electrical stimulation.

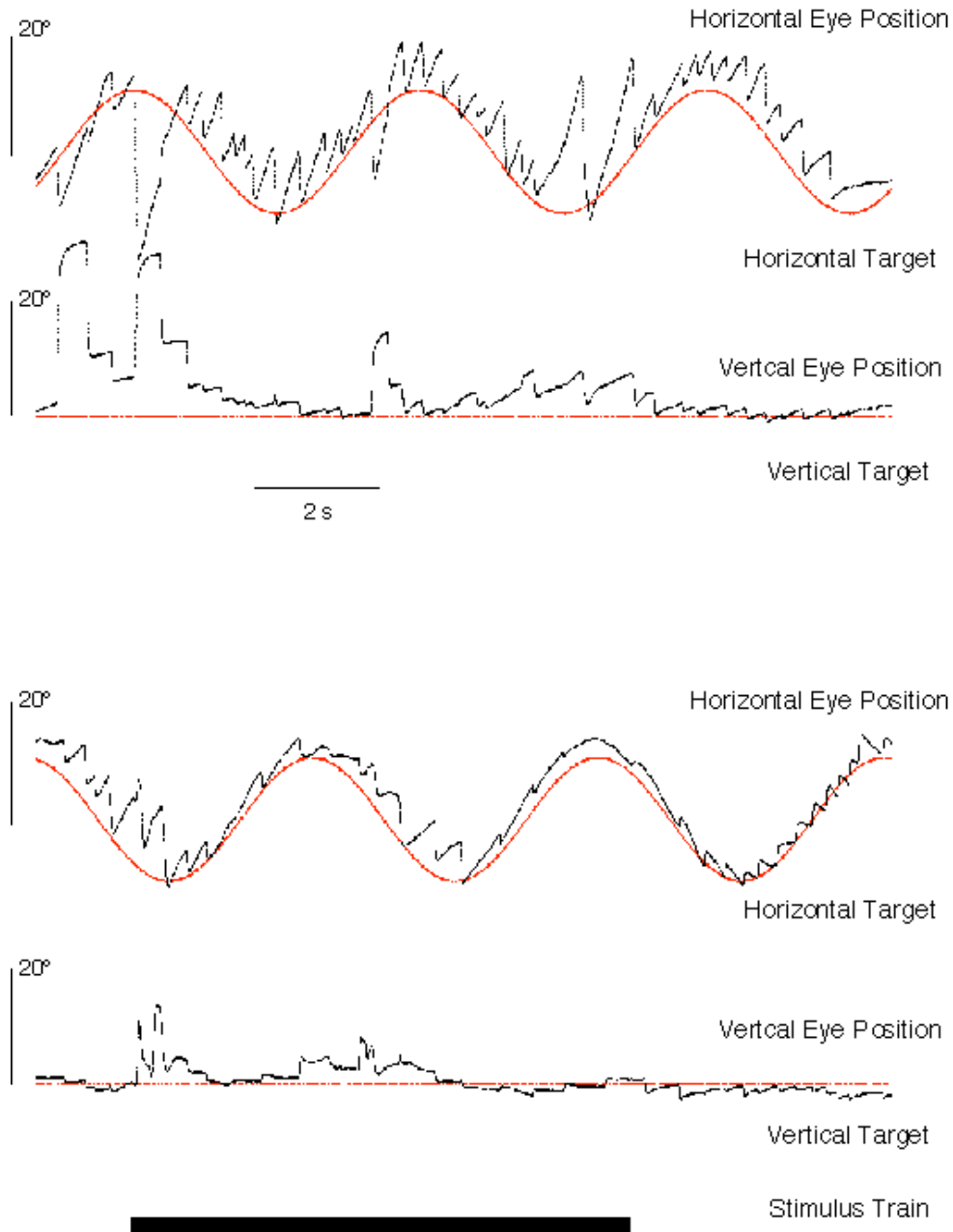
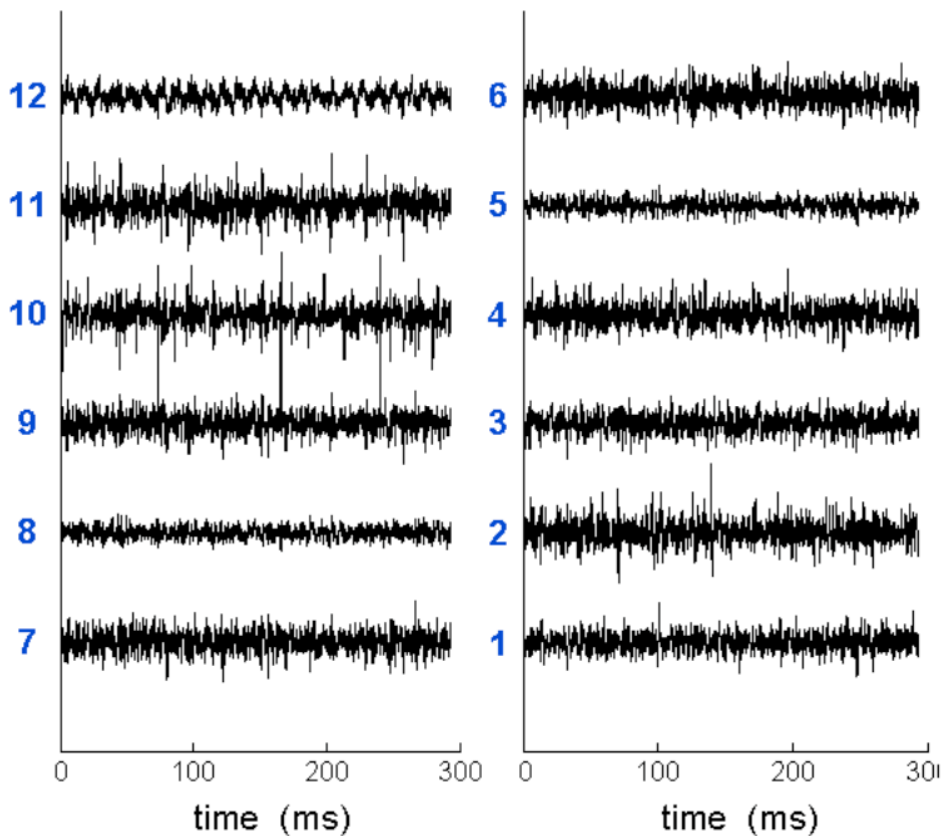


Figure 4: Electrical stimulation during combined pursuit and VOR.

**6. We continued our multiple single unit recording studies, comparing a new tetrode design from Thomas Recording with 12 channel recordings with the Neuronexus-FHC axial array.**

*12 channel recordings.* We continued to evaluate the recording capabilities of the axial array using the two devices we received last quarter. Impedance tests indicated that at least 9 of the 12 sites on each array were functioning. The tungsten electrode tips also had acceptable impedances. Prior to a recording session, all 13 channels (array sites + tip) were iron plated, which previous experience has shown can reduce the level of background noise and movement-related artifacts.



*Figure 5. Axial array recording with an FHC-Neuronexus axial electrode.*

A short recording example from one of the axial electrodes is shown in Figure 5. Three of the array sites (5, 8, and 12) showed no signs of neural activity throughout the experiment, consistent with their high impedances. The other channels exhibited mainly low-level multi-unit activity, with occasional isolated spikes that changed from channel to channel as the electrode was lowered into the brain. In the time segment shown, single-unit spikes are evident on three of the array sites (channels 2, 10, and 11), with the largest appearing on channel 10. This example demonstrates that the axial array can

detect spiking activity on multiple channels simultaneously, which is an improvement over our experience from Quarter 12, in which only one of the twelve channels ever exhibited single-unit spikes. Nevertheless, the quality of the neural activity is poor compared to that of the tungsten electrodes usually used in our lab. We terminated the axial array trials after observing that, on both electrodes, the thin-film layer was peeling away from the tungsten core at the tip. In addition, during two experiments, the animal developed a significant nystagmus with brainstem electrode penetrations.

*Tetrode recordings* We have now acquired multi-channel activity with the Thomas Recording quartz-platinum/tungsten tetrodes in over 20 experiments in 5 animals. Our experience with these devices is positive overall. Occasionally, the quality of single-unit spikes on a single tetrode channel matches the quality obtainable with tungsten microelectrodes. More commonly, the signal-to-noise ratio is lower than with tungsten, so we sacrifice unit isolation for the chance of detecting more than one unit across the four channels. There is a greater tendency with tetrodes to pick up motion artifacts, in particular those caused by the rotation of the animal during natural stimulation of the vestibular system. We will address this issue by revising the connection of the leads and headstage amplifier to the electrode holder.

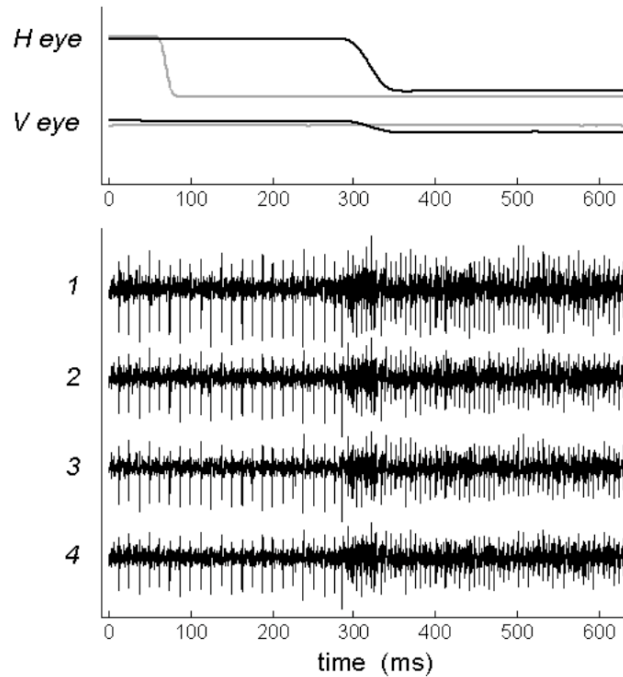


*Figure 6. Example of tetrode recording in the primate brainstem showing multiple records of the same unit.*

Unlike the axial arrays, individual tetrode devices are very robust to day-to-day usage. They are also thinner, and so do not require a larger diameter cannula system. Two examples of tetrode recordings obtained from the same electrode track in the brainstem of a rhesus monkey are shown in Figures 6 and 7. The unit activity in both cases is related



to the monkey's eye movements. In Figure 6, only one isolated unit is apparent, with spikes appearing nearly equally across the four tetrode channels. This situation was fairly common during brainstem recordings, and suggests that the neuron is either large or near the electrode tip (where all recording sites have access to the neuron). This particular neuron displays properties of a left burst tonic brainstem unit.

Figure 7 contains two single units with different eye movement related discharge properties. The larger unit, which appears on channels 2 and 3 (and less so on channel 4), fires a burst followed by an increase in tonic rate when the eye makes a rightward saccade. This is consistent with a right burst tonic neuron. The smaller unit, on channel 4 mainly, has a moderate tonic rate but ceases firing when the eye moves rightward. This unit also discharged a burst of spikes and increased tonic discharge for saccades and subsequent fixation to the left. These firing characteristics are consistent with the properties of a left burst tonic neuron. These two cells were recorded at the anatomic location of the medial margin of the medial vestibular nucleus.

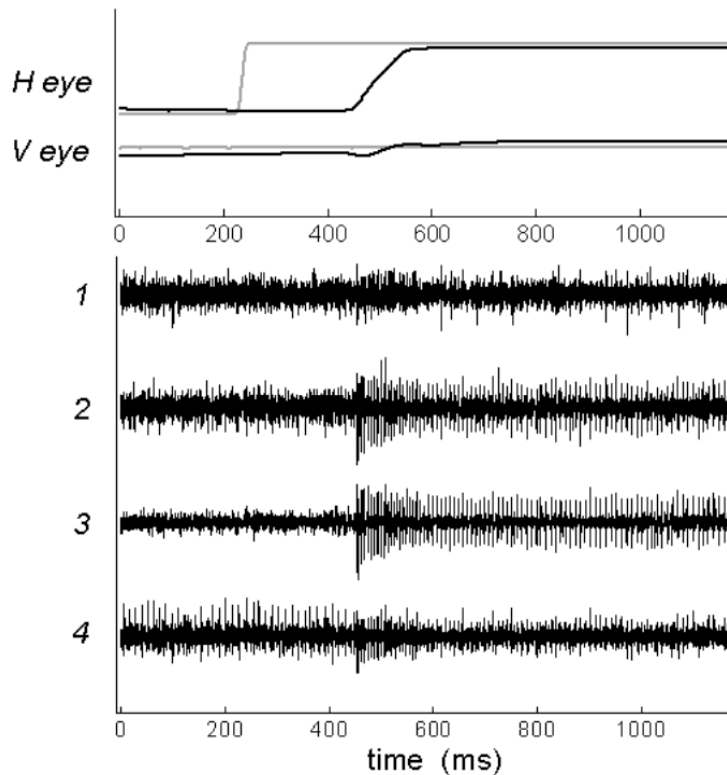


*Figure 7. Example of a tetrode recording in primate brainstem in which two different units are displayed on different channels.*

**7. We continued to record click auditory brainstem responses.** We collected click ABRs in the two newest animals to assess their hearing status prior to any surgical procedure. ABR threshold was defined (see QPR 11) as the minimum click intensity eliciting a clear positive-to-negative excursion above the background noise, usually occurring at a 5 ms latency. Left and right ear thresholds in both animals ranged between

45 and 55 dB SPL (-75 to -65 dB attenuation referenced to a 120 dB calibrated click), comparable to thresholds of normal hearing rhesus monkeys reported in previous studies. This data set will form a baseline for post-surgery ABRs to be measured after implantation of a vestibular prosthesis and recording chamber in each animal.

**8. We started working on the real-time implementation of frequency-modulated pulse trains on the Cochlear SDK development platform.** The SDK cochlear implant interface utilizes a clinical Freedom processor for programming, and Cochlear Corporation provided us all necessary software and hardware for code development. With the platform, we will be able to process head rotational signals in real-time and then transform them into variable-rate stimulation pulse trains. This is a capability not currently available with either the NIC-2 or the clinical Freedom software.

In Quarter 13, we developed test program to demonstrate the feasibility of producing pulse trains on the SDK platform. The program generates simple constant rate and constant amplitude pulse trains. However, producing real-time pulse trains requires an extensive amount of programming work using assembly codes. The Freedom processor has 4 DSP cores running in parallel and, therefore, signal processing tasks must be carefully designed and assigned to each DSP core. Dr. Nie will continue to work one full day per week on programming the research interface in the next quarter.

**9. We continued recording from single neurons in the vestibular nucleus during stimulation with our vestibular prosthesis.** We have made several new observations this quarter, and have substantiated many of our earlier observations. We have shown that there is some variability in electrical stimulation threshold for secondary vestibular neurons, and that higher order units tend to have higher thresholds and typically follow higher frequency stimulation only at current levels well above threshold. More significantly, we continue to encounter neurons with very complex discharge characteristics relative to electrical stimulation. For example, we have observed that there are many neurons that are driven at low frequency, but are silent in response to higher frequency stimulation. These neurons not only fail to follow higher frequency stimulation, but they no longer display a tonic discharge during stimulation.

One such neuron is displayed in Figure 8. In the top panel of Figure 8A, the discharge of the neuron during 10 pps stimulation at 150  $\mu$ A is displayed as a raster aligned on the electrical stimulus artifact (time 0). The unit raster shows individual unit spikes as dots. The blue highlighted dots represent the first unit spike after the onset of a stimulus. This raster shows that most often the neuron in Figure 8A discharges shortly after the stimulus pulse, but occasionally only fires sometime later. These rasters provide a graphical representation of the time locked nature of the neuron discharge with the electrical stimulation at these stimulus parameters. An interesting feature of the discharge is that the unit also appears to show a pause in its spontaneous discharge following the stimulus pulse. To explore the relationship between the elicited spike discharge and the subsequent pause, we performed a current series, reducing the stimulation current in the remaining panels of Figure 8A. As the stimulation current was decreased, the reliability of the short latency spike response in the recorded unit also decreased, producing more

long latency dots indicating a failure to drive the unit (8A middle panel). Finally, at 50  $\mu\text{A}$  (8A lower panel), the unit was no longer driven at short latency, but the pause in activity remained. Because the pause in these units is far longer than a typical interspike interval, we have argued that it is probably an inhibition. We now have further evidence in support of this assertion. As the stimulus current is decreased below threshold for the occurrence of a time locked post stimulus spike (50uA), we see only the presence of a pause. By changing the stimulus current, we have dissociated stimulus evoked pause and the stimulus evoked spike, indicating that the two processes have different stimulation thresholds. The inhibition remains when the stimulation is below the threshold for the excitatory response.

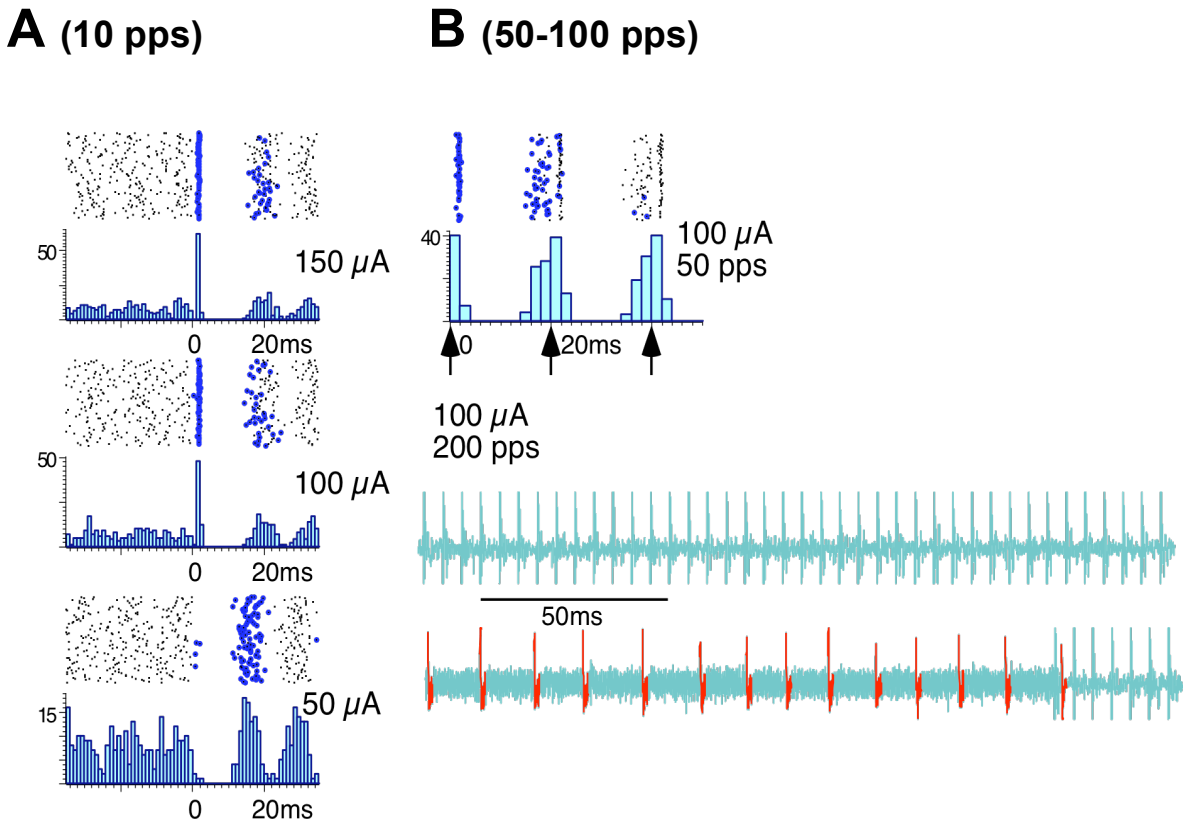


*Figure 8. Unit activity triggered by electrical stimulation of the right lateral canal at varying frequency and current levels. Stimulation parameters are 100  $\mu\text{s}$  per phase and 8  $\mu\text{s}$  gap. A, 3 rasters of 10 pps stimulation at different current levels aligned on the electrical stimulus artifact (time 0). Black dots represent unit discharge, and blue dots represent the first unit spike following the stimulus artifact. B, Upper panel, a raster of unit discharge at higher stimulation frequency and 100  $\mu\text{A}$  current. B, lower traces, unit discharge (red) and stimulus artifact (grey) during and before electrical stimulation at 200 pps and 100  $\mu\text{A}$  current.*

This result has very important consequences for the unit discharge during higher frequency stimulation. For example, the discharge of the neuron during 50 pps stimulation at 100  $\mu\text{A}$  is displayed in the upper panel of Figure 8B as a raster. The raster

shows that most often the neuron in Figure 8B discharges shortly after the stimulus pulse (time 0, first vertical arrow), but occasionally only fires sometime later, typically before the next stimulus (second vertical arrow) and always before a third stimulus pulse has occurred (third vertical arrow). These rasters indicate that at 50 Hz and 100  $\mu$ A the unit discharge is still time locked to the electrical stimulus artifact. However, in the bottom panels, we show the result of stimulation at 200 Hz and 100  $\mu$ A in the same unit. In the upper of the two unit traces, we show only the stimulus artifact associated with the electrical stimulus train at 200 Hz, and 100  $\mu$ A. This is because there is no unit discharge recorded at this time, although the unit remains isolated. The lower unit trace shows the onset of the stimulation. The unit discharge in red is clearly visible until the high frequency stimulation, and stimulus artifact, begins. At that point the unit ceases to fire, presumably because of the effects of the inhibitory input demonstrated earlier. Therefore, this unit is responding during both low and high frequency stimulation, but the responses are dominated by the short latency excitatory response at low stimulation frequency, and the longer latency inhibitory response at higher stimulation frequencies. This is a very interesting and unexpected characteristic of the observed neural discharge in response to electrical stimulation with our implanted vestibular prosthesis.

#### **Objectives for Quarter 14:**

- 1. We will continue our recording studies, focusing on the relationship of unit discharge and stimulus current and frequency in vestibular nucleus neurons.**
- 2. We will meet with the FDA to discuss our pre-IDE, in preparation for the submission of a full IDE application to the FDA for extension of our studies to human subjects.**
- 3. We plan to receive and use our first axial multi-electrodes from Lawrence Livermore. Until that time we will continue to use the Thomas Recording tetrodes.**
- 4. We will continue to develop real time frequency modulated stimulation, to complement the real time amplitude modulated stimulus that we are currently evaluating.**
- 5. We will continue parametric studies of gain modulation of the VOR with real time modulated electrical stimulation.** Specifically, we will evaluate the rotational frequency and velocity dependence of this phenomenon.
- 6. We will begin to collect histological data for analysis of the implant orientation within the end organ using spiral CT.** We will also submit a proposal to NIDCD for the further study of temporal bone specimens with micro-CT and histological reconstruction of embedded decalcified temporal bone sections.